ACS ES&T Engineering

pubs.acs.org/estengg

Article

Investigation of Hydronium Diffusion in Poly(vinyl alcohol) Hydrogels: A Critical First Step to Describe Acid Transport for Encapsulated Bioremediation

Carson J. Silsby, Jonathan R. Counts, Thomas A. Christensen, II, Mark F. Roll, Kristopher V. Waynant, and James G. Moberly*

Cite This: https://doi.org/10.1021/acsestengg.2c00107

Read Online

ACCESS | Metrics & More | Article Recommendations | Supporting Information

ABSTRACT: Bioremediation of chlorinated aliphatic hydrocarbon-contaminated aquifers can be hindered by high contaminant concentrations and acids generated during remediation. Encapsulating microbes in hydrogels may provide a protective, tunable environment from inhibiting compounds; however, current approaches to formulate successful encapsulated systems rely on trial and error rather than engineering approaches because fundamental information on mass-transfer coefficients is lacking. To address this knowledge gap, hydronium ion mass-transfer rates through two commonly used hydrogel materials, poly(vinyl alcohol) and alginic acid, under two solidification methods (chemical and cryogenic) were measured. Variations in hydrogel crosslinking conditions, polymer composition, and solvent ionic strength were investigated to understand how each influenced hydronium ion diffusivity. A three-way ANOVA indicated that the ionic strength, membrane type, and crosslinking method significantly ($p < 0.001$) contributed to changes in hydronium ion mass transfer. Hydronium ion diffusion increased with ionic strength, counter to what is observed in aqueous-only (no polymer) solutions. Co-occurring mechanisms correlated to increased hydronium ion diffusion with ionic strength included an increased water fraction within hydrogel matrices and hydrogel contraction. Measured diffusion rates determined in this study provide first principal design information to further optimize encapsulating hydrogels for bioremediation.

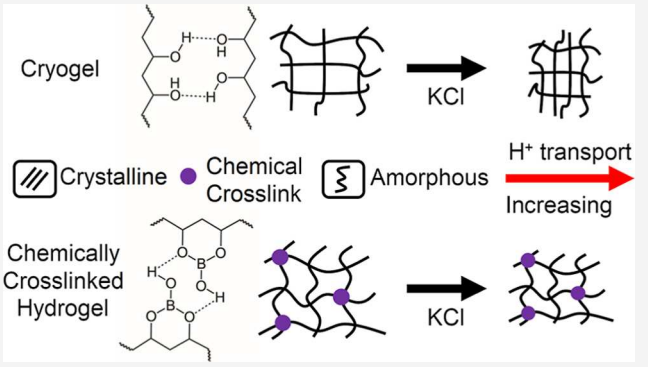

KEYWORDS: *hydronium ion diffusion, mass transfer, hydrogel, crosslinking, ionic strength*

INTRODUCTION

Remediation of chlorinated aliphatic hydrocarbons (CAHs), such as trichloroethylene (TCE), are primary or co-contaminants in over 50% of superfund sites and brownfields across the United States.[1,2] Bioremediation of CAHs by anaerobic reductive dechlorination is one potential remediation technique being researched at the lab scale[3−6] and in the field.[7−9] Microbial consortia are key players in bioremediation due to their ability to chemotax toward contaminant sources in the environment, act as self-replicating catalysts, degrade contaminants to low regulatory requirements, and provide low-cost treatment compared to other methods. However, Robinson *et al.*[10] demonstrated that metabolically generated acids in poorly buffered systems could severally inhibit microbial consortia and stop the degradation process before complete dechlorination was achieved. Yu and Semprini[11] and Haest *et al.*[12] also showed that microbial anaerobic reductive dechlorinators were inhibited by CAHs, which lead to a decreased dechlorination efficiency and incomplete dechlorination in highly contaminated areas. Halting dechlorination prior to complete degradation of vinyl chloride may leave the system in a more toxic state; therefore, processes that protect microorganisms from inhibitory conditions may improve the efficiency of microbial anaerobic reductive dechlorination.

Accumulation of acids generated during each step of anaerobic reductive dechlorination of CAHs can also inhibit biodegradative processes. Puentes Jácome *et al.* determined that the biological rates of reductive dechlorination for *Sporomusa* sp. KB-1 were inhibited at pH 5.5 and ceased at 5 or below.[4] Natural microbial processes (alkalinity generation) or buffers within groundwater systems can protect organisms for a time but may be overwhelmed. Once natural buffers within groundwater were depleted, Robinson *et al.*[10]

Received: April 2, 2022
Revised: August 19, 2022
Accepted: August 22, 2022

found that acid neutralizers were required at 2−13 times the amount of contaminant dechlorination, and without frequent reinjection of neutralizers, remediation would fail. Common acid neutralizers include bicarbonate, carbonate, sodium hydroxide, lime, and silicate.[10,13]

Biofilms, flocs, and multicellular clusters are natural forms of encapsulation used to control transport and are one of the means by which microorganisms have adapted to a wide variety of environmental conditions including extreme pH changes.[14] A potential solution to toxic acid accumulation and high contaminant concentrations is to artificially encapsulate microorganisms in a biocompatible hydrogel or "biobead".[15,16] Hydrogels, the primary material for biobead encapsulation, are three-dimensional matrices formed by polymer chains cross-linked into a cage-like structure separated by water domains.[17] Biobeads provide a microenvironment for better native and localized control of acid by microorganisms and protection from inhibition by environmental toxins, including CAHs. Additionally, biobeads can be modified to include buffers and other passive and active compounds (*e.g.*, zero-valent metals, activated carbon).[18] Studies by Zhou *et al.*,[19] Wang and Tseng,[20] and Kim *et al.*[21] each used encapsulated microorganisms for the dechlorination of TCE and its biproducts; however, all studies utilized buffering compounds to maintain pH ∼7 during dechlorination. To the authors' knowledge, no studies to date have evaluated the ability of encapsulating hydrogels to protect microbes *in vitro* or *in situ* without buffers or where system buffering was overwhelmed. An additional knowledge gap toward engineering these hydrogel materials for remediation is a lack of published fundamental mass-transfer constants (diffusivity) of key metabolites, waste products (acid), and contaminants, which would allow for development of reaction−diffusion-type computational models, proper geometry sizing, and materials tuning to match biological degradation rates of contaminants to mass-transfer rates. Consumption of TCE and complete breakdown to ethylene or CO_2 requires a balance of both reaction rate (governed by the microorganism growth rate and metabolism of each constituent) and mass transfer (governed by bead size, polymer properties, diffusivity of constituents) to the microbial self-replicating "catalysts". Optimal conditions balance reaction and mass transfer of CAHs, acid, and nutrients so that CAHs and hydronium mass transfer are kept at a level where inhibition is minimal, and nutrients are supplied in sufficient quantities to maintain growth conditions. Determining CAH and nutrient effective diffusion coefficients is also critical, but hydronium diffusion will be the main focus of this study because fundamentally, regulation of pH is the most critical priority of microorganisms because it directly impacts all metabolic processes. Microorganisms resist pH change through a variety of internal means (*e.g.*, proton efflux or accumulation, reactions to form neutral chemical species and buffering compounds, control of membrane permeability to restrict transport) but at the cost of metabolic energy and optimal growth.

Polymer domains within hydrogels are made up of amorphous and crystalline regions. Crystalline regions are impermeable to solute diffusion and have been shown to hinder solute diffusion, while amorphous regions are more flexible but act as roadblocks to solute diffusion. Poly(vinyl alcohol) (PVA) hydrogels are commonly used in cryogel and chemically crosslinked hydrogel studies.[22−31] Previous work by Schuszter *et al.*[22] investigated hydronium diffusion in non-PVA hydrogels, and Choudhury *et al.*,[23] Ajith *et al.*,[24] and Wang *et al.*[32] measured hydronium conductivity in PVA hydrogels but did not quantify hydronium diffusivity, a critical knowledge gap in these materials. NMR analysis of hydronium diffusion in aqueous systems is common, but this technique is infeasible in hydrogel systems because the high water content in the hydrogel would mask the hydronium signal.[22]

Describing mass transfer of acid (*e.g.*, hydronium ions) in hydrogels, especially under different environmentally or biologically relevant conditions, is a critical first step needed to design first-principle models of CAH dechlorination using biobeads and to better understand how physical changes within a hydrogel may alter mass-transfer rates.

Previous mass-transfer research has explored three areas of distinct overlap with this study: scaling models of general diffusion in hydrogels,[33] the diffusivity of hydronium ions in electrolytes,[34,35] and structural hydrogel changes in electrolyte solutions.[29,36,37] Generally, for most molecules, Brownian motion describes the mechanism of mass transport in hydrogels influenced by polymer−solute and/or polymer−solvent−solute interactions. However, hydronium ions possess a unique propagation pathway, the Grotthuss mechanism,[38] or "proton hopping", which greatly enhance hydronium ion diffusion above Brownian motion.

Solution and hydrogel interactions at interfaces may also influence hydronium diffusion. Roberts[35] found that hydronium diffusion was suppressed in electrolyte solutions, while Roberts and Zundel[39] reported hydronium diffusion was enhanced at quartz surfaces. With the potential for multiple mechanisms to influence hydronium diffusion in hydrogels, this study seeks to define hydronium effective diffusivities in blends of PVA and alginic acid (Alg) hydrogels under solutions of different ionic strengths to encompass a wide range of potential groundwater types where these materials may be used. Additional evaluated design factors included the effects of PVA weight per volume fraction and crosslinking method. Experimental results were compared with theoretical predictions of hydronium ion diffusion using scaling law models.[33] This study provides fundamental mass-transfer constants critical for first principal design of biobeads.

MATERIALS AND METHODS

Reagents. Alg, 98.0−98.8% hydrolyzed PVA (molecular weight: 31−50k, 85−124k, and 146−186k Da) powders, 99% potassium chloride, and calcium chloride were obtained from Sigma-Aldrich. Food-grade sucrose was obtained from a local grocery store. Trace metal grade hydrochloric acid from Fisher Scientific was diluted with house-distilled and deionized water to pH 2.35. Technical grade boric acid was obtained from ChemProducts. All chemicals were used without further purification. NIST traceable pH standards (Fisher) were used to calibrate pH probes before each diffusion run.

Polymer Crosslinking. 10% PVA−2% alginate (10% PVA/2% Alg) polymers were prepared as follows: 10.0 g of PVA (MW: 146,000−186,000 Da) was added to 100 mL of deionized water and heated to 80 °C with vigorous stirring. Once PVA was dissolved, 2.0 g of Alg polymer was added to the mixture and held at 80 °C while the solution reached a homogeneous consistency. Hydrogel-blended polymer solutions were transferred to disc-shaped casting molds, frozen at −20 °C, and crosslinked by sequential freeze/thaw cycles as done previously by Holloway *et al.*[40] These hydrogels which are also known as "cryogels" were used as a comparative

https://doi.org/10.1021/acsestengg.2c00107
ACS EST Engg. XXXX, XXX, XXX−XXX

control. A cycle consisted of thawing a frozen hydrogel for 1 h at room temperature and then refreezing at −20 °C for 1 h. After five repeated cycles of freezing and thawing, the hydrogel formed dense crystallized domains which prevented polymer dissolution in water.[40] No crosslinking agents were added to these cryogels. PVA hydrogels from 7 to 15% were prepared with 146−186 kDa PVA, while 20% cryogels were from 85 to 124 kDa PVA, and 30% hydrogels were from 31 to 50 kDa PVA due to aqueous solubility limits.

Alternatively, after initially freezing the casted gel for at least 1 h, the hydrogel was submerged in an ionic crosslinking solution at 4 °C for 4−8 h and repeatedly rinsed with deionized water to remove excess crosslinking agents, similar to the preparation of biobeads by Wu and Wisecarver.[41] Unless otherwise stated, blends of PVA/Alg hydrogels were crosslinked using an aqueous saturated boric acid solution with 2% (w/v) calcium chloride. Non-blended PVA hydrogels were crosslinked using only saturated boric acid. Prior to measuring diffusion, all hydrogels were pre-equilibrated in deionized water, 0.1 M sucrose, or 0.001−1 M KCl solution for at least 2 h, in accordance with the solute−solvent used in the experiment.

Variation of Solvent Ionic Strength. Diffusive measurements were conducted in solutions with ionic strengths ranging from 0 to 1 M using KCl as the ionic species in water. Sucrose was used as a non-ionic alternative to KCl.

Apparatus for Diffusion Measurements. The diaphragm cell method was used to quantify effective diffusivity of hydronium through hydrogels. This method separates a "source" solution containing the solute of interest from a "sink" chamber by a thin diaphragm or hydrogel membrane. Detailed diagrams of the apparatus can be found in the Supporting Information (Figures S1 and S2). Constant stirring of both the sink and source chambers minimizes mass-transfer limitations and boundary layer effects. The concentration of the solute in the sink was monitored over time and related to effective diffusivity by Fick's first law and the definition of flux. The mathematical derivation using the diaphragm cell is shown in more detail by Northrop and Anson[42] and provided in the Supporting Information.

The concentration in the sink chamber was measured using pH probes (Oakton). To enable simultaneous triplicate pH measurements, a diaphragm cell was constructed of PVC pipes with three sinks connected to a single larger source. The final source pH was measured using a commercial benchtop pH meter (Hach H170) and pH probe (Accumet). Final sink pH values were recorded and used to correct instrument drift (see the Supporting Information). Both the source and sink were unbuffered to provide a maximum concentration driving force and avoid interference of counter diffusing species once protonated. The source pH remained nearly constant (<0.5% concentration difference) over the course of the entire experimental measurement.

Theoretical Hydronium Diffusion. To estimate hydronium diffusion through PVA membranes, the scaling law developed by Lustig and Peppas was employed to normalize the diffusion coefficient.[33] Calculations were only completed for 10% PVA hydrogels due to model limitations for single-component hydrogels. Swelling experiments, requisite for estimating parameters for the model, were performed to determine the swelling behavior of the hydrogels after crosslinking. Membranes were cast and crosslinked as described above. The volume of each hydrogel was calculated using the known cross-sectional area of each casting mold and measuring the average equilibrated thickness of the membranes from five spatial points after swelling. The polymers were dried in a vacuum oven at 40 °C until no weight change was observed. Physical parameters were calculated using eqs S4−S7 as described by Meadows and Peppas[43] and Peppas and Merrill.[44] The mesh size of the swelled polymer gel was calculated using eq 1,[45] where Q is the degree of swelling (eq S5), C_n is the Flory characteristic ratio (8.3 for PVA), N is the number of links between repeating units per poly chain (eq S7), and l is the (C−C) bond length across the polymer chains (1.54 Å for PVA)[45]

$$\xi = Q^{1/3}(C_n \cdot N)^{1/2} l \tag{1}$$

The normalized diffusion coefficient was determined using the scaling law as defined by Lustig and Peppas,[33] where subscripts α, β, and γ denote water, polymer, and solute, respectively

$$\hat{D} = \frac{D_{\gamma,\alpha\beta}}{D_{\gamma,\alpha}} \cong \left[1 - \frac{r}{\xi}\right] e^{\left[-\frac{Y}{(Q-1)}\right]} \tag{2}$$

$\hat{D}$ is the normalized diffusion coefficient, $D_{\gamma,\alpha\beta}$ is the diffusion coefficient of the solute through the hydrogel, $D_{\gamma,\alpha}$ is the diffusion coefficient of the solute through water, r is the Stokes hydrodynamic radius of the solute (2.82 Å H_3O^+,[46] 3.58 Å Na^+,[46] 1.30 Å H_2O[47]), and Y is a structural parameter (assumed to equal 1 as an approximation)[33]

$$WC = \frac{\frac{\rho_p}{\rho_w}\frac{w_w}{w_p}}{1 + \frac{\rho_p}{\rho_w}\frac{w_w}{w_p}} \tag{3}$$

The hydrogel water content was calculated as done previously by Ajith *et al.*[24] and is shown in eq 3, where w_w and w_p are the weight of water in the hydrogel after swelling and the hydrogel dry weight, respectively. ρ_w and ρ_p are the densities of the hydrogel equilibration solution and of the initial polymer, respectively (*i.e.*, PVA or a weighted average of PVA and Alg). The densities of electrolyte solutions were calculated using linear interpolation of experimental data reported by Zhang and Han.[48]

Previous work by Wraight[49] used sodium as a surrogate for hydronium. The size and charge of a sodium ion is comparable to those of hydronium, allowing for the estimation of diffusive properties of hydronium through a hydrogel without the enhanced transport provided by the Grotthuss mechanism. For comparison, the diffusion coefficients used as parameters in eq 2 were hydronium ($D_{\gamma,\alpha} = D_{e(H_3O^+,aq)} = 9.3 \times 10^{-5}$ cm^2/s),[49] sodium ($D_{\gamma,\alpha} = D_{e(Na^+,aq)} = 1.33 \times 10^{-5}$ cm^2/s),[49] and water ($D_{\gamma,\alpha} = D_{e(H_2O)} = 1.73 \times 10^{-5}$ cm^2/s).[47] Additional models relevant to solute diffusion in hydrogels have been reported by Masaro and Zhu.[50]

A sensitivity analysis of parameters used in the Lustig and Peppas model was also performed for solution conditions of 0, 0.1, and 1 M KCl in both chemically crosslinked and cryogel forms from at least triplicate hydrogel samples (included as the Supporting Information). Adjusted parameters for sensitivity analysis included polymer structural parameter, Flory characteristic ratio, Flory interaction parameter, specific volume of polymer repeating unit, and Stokes hydrodynamic radius of the diffusing species.

https://doi.org/10.1021/acsestengg.2c00107
ACS EST Engg. XXXX, XXX, XXX−XXX

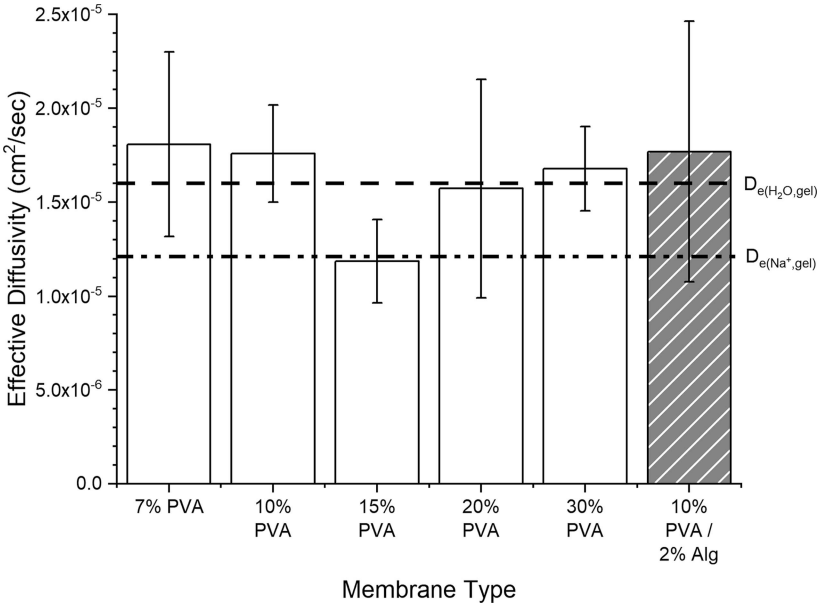

Figure 1. Effective diffusivity of hydronium through cryogels of various polymer compositions. Statistical analysis showed that 15% PVA was the only significantly different membrane composition when compared with 7, 10, and 30% PVA. The horizontal lines represent calculated self-diffusion of the given species in a 10% PVA cryogel. Error bars represent a 95% confidence interval.

NMR Analysis. ^{1}H and ^{11}B NMR analyses were completed using a Bruker AVANCE III 500 spectrometer equipped with a Prodigy cold probe. The frequency used for ^{1}H NMR was 500.13 and 160.47 MHz for ^{11}B NMR. All spectra were collected at +30 °C. ^{11}B NMR spectra were collected in quartz NMR tubes, but due to the presence of borosilicate glass on the instrument probe, further corrections were required. To remove the broad borosilicate glass peak, a blank D_2O spectrum was subtracted from each sample spectrum. All NMR and Raman experiments were completed using 2,4-pentanediol as a substitute for PVA as done previously by Itou *et al.*[25] to avoid polymerization. Samples were prepared by dissolving 2,4-pentanediol, boric acid, and potassium chloride in D_2O. Sodium hydroxide was used to adjust pH. Samples varying ionic strengths were 10% 2,4-pentanediol in saturated boric acid and 0, 0.001, 0.5, and 1 M KCl. Samples studying the effects of changing pH were composed of 0.23 M 2,4-pentanediol and 0.02 M boric acid. Sodium hydroxide was added until a pH of 9 was achieved, similar to a preparation done by Sinton.[51]

Raman Spectroscopy. Raman spectroscopy was completed using a WITec alpha300 Raman microscope with a UHTS-300 spectrometer and a 1600 × 200 pixel CCD array detector. A 532.53 nm laser source was used with a nominal 100 mW (max) power manually adjusted for an appropriate signal-to-noise (baseline) quality below 15 mW incident through a 20× objective (Nikon). Reported spectra represent the control software averages of 10 spectral accumulations each acquired at 0.5 s integration times. Data were analyzed using WITec Control FOUR software v4.1. Equimolar liquid samples were prepared with combinations of 2,4-pentanediol, boric acid, and potassium chloride in DI water.

FTIR Spectroscopy. FTIR analysis was done using a Nicolet 6700 FTIR spectrometer (Thermo Scientific) with a circle liquid analyzer (0005-105, Spectra Tech Inc.) attachment. Spectra were collected between 650 and 4000 cm^{-1} with a resolution of 4 cm^{-1} by averaging 32 scans and analyzed using OMNIC software v8.3. Liquid samples were prepared as described in the Raman Spectroscopy section.

X-Ray Diffraction. X-ray diffraction (XRD) analysis was done using a Bruker D8 XRD equipped with a 2-D detector and a copper X-ray tube (1.54056 Å). A collimated X-ray beam of 500 μm was used to collect data. Spectra were collected in four separate frames at 300 s per frame for a total scan range of 6−95°. Samples were prepared as mentioned in the polymer crosslinking section above and then dried at room temperature before analysis; the samples did not undergo any further modification.

Data Analysis. Diffusion experiments were performed in triplicate at a minimum. Reported values of hydronium diffusion in hydrogel were the compiled average of these measurements, with error bars representing a 95% confidence interval. Comparisons between values were conducted using a two-sample *t*-test in OriginLab 2018b (OriginLab Corporation, MA) and adjusted using Holm's correction in R (v4.1.1).[52] R packages car,[53] multcomp,[54] phia,[55] afex,[56] and emmeans[57] were used for data analysis. Group comparisons were done using type II analysis of variance (ANOVA) in R with all results considered statistically significant at the 95% confidence level ($p < 0.05$). Diffusion coefficient calculations follow Northrop and Anson[42] and are presented in more detail in the Supporting Information (eqs S1 and S2).

RESULTS AND DISCUSSION

Diffusion of solutes through hydrogels is influenced primarily by physical obstruction from the polymer, electrostatic effects, and polymer−solute chemical interactions such as hydrogen bonding.[58−60] In order to separate some of these effects and gain insights into mass-transfer mechanisms, diffusion measurements were performed in single-component gels (*e.g.*, 10% PVA), multicomponent gels (*e.g.*, 10% PVA/2% Alg), different solidification methods (*e.g.*, cryogels *vs* chemical crosslinking), and different ionic strengths. Each treatment set is addressed individually below.

https://doi.org/10.1021/acsestengg.2c00107
ACS EST Engg. XXXX, XXX, XXX−XXX

Influence of the Crosslinking Method on Hydronium Diffusion—Cryogels. The aqueous hydronium ion diffusivity as reported by Agmon[38] and Wraight[49] was 81.1% faster than the measured diffusivity in 10% PVA cryogels, 1.76×10^{-5} cm^2/s. Schuszter *et al.*[22] calculated hydronium ion diffusivity in agarose hydrogels within the same order of magnitude. A reduction in hydronium effective diffusivity relative to pure water may be explained by physical obstruction by polymer domains within the hydrogel including impermeable crystalline regions.[30,61] Polymer chains, which make up the hydrogel structure, act as road blocks to diffusing species as they move between water domains. Two physical parameters which may exacerbate obstruction within the hydrogel are polymer mass fraction and crystallinity.

Increasing the polymer mass fraction increases the density of polymer chains within a membrane, which decreases the free volume of the hydrogel and presents a higher possibility for obstruction to diffusion. To examine whether polymer mass fraction influenced hydronium transport, several different PVA-blended cryogels were evaluated. Several PVA molecular weights were used to accommodate solubility limits (see the Materials and Methods section), but the effects of PVA molecular weight on hydronium diffusivity were not investigated.

Figure 1 depicts the effective diffusivity of hydronium through several PVA hydrogel blends. Statistical analysis of Figure 1 was completed using the Tukey method to compare individual means. 15% PVA was the only polymer composition that had significantly different hydronium diffusivity when compared to any of the other PVA compositions. Hydronium diffusion through 15% PVA was statistically significant when compared to 7% ($p = 0.002$), 10% ($p = 0.002$), and 30% PVA ($p = 0.008$); all other combinations were not significant. Molecular weight likely had an effect on hydronium diffusivity in the hydrogels tested due to variations in chain length and mobility corresponding the PVA used in each hydrogel blend. Chain mobility can make crystallization more favorable due to chain movement during crystallite formation. Hydronium diffusivity in 20 and 30% PVA cryogels was likely only similar to that in 10% PVA cryogels due to the decrease in PVA molecular weight. Additional low-molecular weight PVA added to the hydrogel mixture to make 20 and 30% PVA likely made the polymer density close enough to 10% PVA to make the diffusivity behavior similar.

Considering the impact of crystallinity on changes in diffusivity, increases in polymer mass fraction, regardless of molecular weight, may lead to an increase in crystallinity due to the increasingly close proximity of polymer chains as more polymer is added to the hydrogel blend. With more polymer chains present, the chains are simply more likely to be pushed together during crystal formation, making the development of crystalline regions more favorable. The formation of crystalline regions increases obstruction to diffusion in a hydrogel because crystalline regions are impermeable to solute diffusion[30,62] in comparison to amorphous regions where solute molecules can simply navigate around polymer chains within the hydrogel. In a study done by Holloway *et al.*,[40] using a PVA molecular weight similar to that of the 20% PVA cryogels in this study, researchers found that the crystallinity of 30% PVA cryogels was 10 times that of 10% PVA.

While fully assessing gel crystallinity was beyond the scope of this study, we note that polymer molecular weight can also affect the formation of crystalline domains within the hydrogel due to chain length. For the same mass fraction, a higher-molecular weight polymer will provide fewer but longer chains, while a lower-molecular weight polymer will be made up of additional shorter chains. Shorter polymer chains will be expected to have significantly more mobility to adopt a crystalline conformation in comparison to highly entangled, long polymer chains. This is the hypothesized reason for the drop in diffusivity when the PVA polymer composition was increased to 15% PVA using the high-molecular weight PVA, a mass fraction which was approaching the solubility limit. The hydronium diffusivity decreases from 10 to 15% PVA, indicating that obstruction may be caused by chain entanglement and a larger proportion of amorphous polymer gel. A similar trend would be expected when using lower-molecular weight PVA at polymer mass fractions approaching the solubility limit. Clearly, additional studies into the effects of PVA molecular weight on crystallinity and hydronium diffusion, with a complete assessment of the fraction of crystallinity using the methods of Ricciardi *et al.*,[63] would be beneficial for better understanding these mechanisms.

Interestingly, when testing whether the number of freeze/thaw cycles would have an effect on hydronium diffusivity, no significant difference was found between 10% PVA cryogels crosslinked with between two to five freeze/thaw cycles ($p = 0.3857$, Figure S5). Holloway *et al.*[40] calculated the relative crystallinity of PVA cryogels (10, 20, 30, 35% PVA) prepared by similar procedures, with lower-molecular weight PVA, and found that the crystallinity of 10% PVA cryogels increased by less than 1% after over five freeze/thaw cycles. However, the relative crystallinity of 30% PVA cryogels increased by about 2% after the same number of cycles, which, along with the experimental results previously discussed, indicates that PVA volume fraction, and therefore hydrogel polymer density, had a greater effect on hydrogel crystallinity and hydronium diffusivity than the number of freeze/thaw cycles.

Influence of the Crosslinking Method on Hydronium Diffusion—Chemically Crosslinked Hydrogels. To examine the combined effects of polymer and crosslinking chemical constituents on hydronium diffusivity, chemically crosslinked PVA and PVA/Alg hydrogels were studied. Cryogels were used as control groups for comparison purposes to elucidate the effects of introducing additional chemical constituents into the hydrogel as done previously by Patachia *et al.*[64] Significant differences in hydronium effective diffusivities were observed between hydrogels crosslinked by chemical reagents (Figure 2a–e) and freeze/thaw cycles (Figure 2f,g). Boric acid crosslinked 10% PVA hydrogels (Figure 2a) had an effective diffusivity that was 58% higher than that of 10% PVA cryogels ($p = 0.002$, Figure 2f). Crosslinking 10% PVA/2% Alg hydrogels with calcium chloride and boric acid for 4.5 h (Figure 2b) decreased the hydronium diffusivity by 47% ($p = 0.03$) when compared to the equivalent cryogel (Figure 2g). Calcium ions integrated into the polymer network may have electrostatically repelled hydronium ions, decreasing hydronium's effective diffusivity by inhibiting the transport efficiency. Longer crosslinking times (4.5 *vs* 6.5 and 8 h) for 10% PVA/2% Alg hydrogels increased the measured effective diffusion rates ($p = 0.004$) as shown in Figure 2b–d potentially due to increased boric acid crosslinking. After chemically crosslinking for at least 6.5 h, 10% PVA/2% Alg hydrogels had an effective diffusivity similar (~0.003% difference, $p = 1$) to the equivalent cryogel. Alternatively, when crosslinked for 4.5 h with only boric acid (Figure 2e), 10% PVA/2% Alg hydrogels

https://doi.org/10.1021/acsestengg.2c00107
ACS EST Engg. XXXX, XXX, XXX−XXX

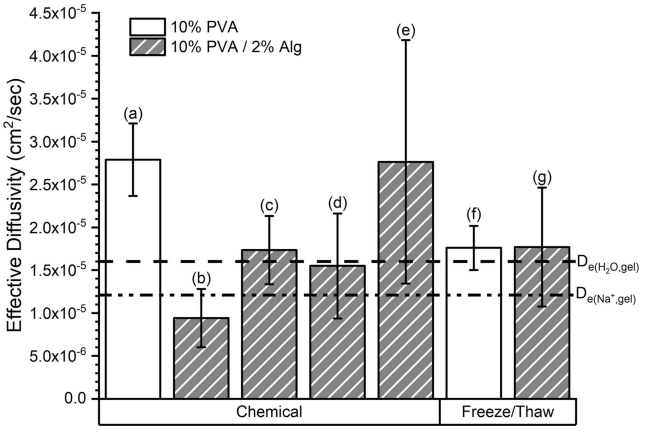

Figure 2. Effective diffusivity of hydronium in chemically crosslinked 10% PVA and 10% PVA/2% Alg hydrogels, crosslinked by different methods. Numbers indicate different crosslinking methods: (a) 10% PVA crosslinked for 4.5 h in saturated boric acid, (b) 10% PVA/2% Alg crosslinked for 4.5 h in 2% $CaCl_2$ and saturated boric acid, (c) 10% PVA/2% Alg crosslinked for 6.5 h in 2% $CaCl_2$ and saturated boric acid, (d) 10% PVA/2% Alg crosslinked for 8 h in 2% $CaCl_2$ and saturated boric acid, (e) 10% PVA/2% Alg crosslinked for 4.5 h only in saturated boric acid, (f) 10% PVA cryogel, and (g) 10% PVA/2% Alg cryogel. The horizontal lines represent calculated self-diffusion of the given species in a 10% PVA cryogel. Error bars represent a 95% confidence interval. Average diffusivity and error values for each data point can be found in Table S5.

performed identically (~0.009% difference, $p = 1$) to 10% PVA treated in a similar fashion (Figure 2a). This suggests that in the absence of the calcium crosslinker, Alg acts as a passive component in the hydrogel blend with no additional crosslinking behavior.

The stark differences observed between effective diffusivities in Figure 2 may be due to these co-occurring factors: (1) chemically crosslinking PVA with boric acid prevented the formation of crystalline PVA−PVA structures, allowing the membrane to expand water domains and increase hydronium diffusivity (Figure 2a,f and e,g), (2) the formation of PVA−borate complexes increased the acidity of the hydrogel environment and improved the ability of the hydrogel to transport protons, and (3) electrostatic repulsion by calcium ions bonded to Alg (Figure S7) decreased hydronium diffusivity. Factor 1 is supported by Huang *et al.*,[65] who state that boric acid crosslinking decreases hydrogel crystallinity, allowing for additional water uptake and water domain expansion. Crystallinity hinders water uptake by binding polymer chains together with hydrogen bonds, therefore restricting hydrogel expansion. When boric acid crosslinks PVA chains, the resulting complex prevents hydrogen bonding by separating polymer chains with a rigid structure. Even though the PVA−borate complex is rigid, the polymer chains are amorphous after crosslinking and so unlike crystalline regions are far more flexible and present less obstruction to solute transport. Water content experiments (shown in Table 1) further support factor 1 and the results described by Huang *et al.*[65] as the water content significantly increased from 94.1 to 95.8% in 10% PVA hydrogels ($p = 0.003$) when chemically crosslinked. Water domain expansion is expressed by an increase in water content since more water occupies the hydrogel volume. As water domains expand, the hydrogel swells and the relative space occupied by polymer chains decreases, making it easier for solute molecules to traverse the hydrogel and avoid obstruction from polymer domains. Similar results were reported by Gayet and Fortier,[66] who determined that an increase in water content led to more efficient mass transport due to less obstruction from polymer domains. Factor 2 is supported by Rietjens and Steenbergen,[67] who demonstrated that complexed borate, like the complex shown in Figure 3c, is strongly acidic due to ring strain (C−O−B−O−C−C). Factor 2 can also be supported by aqueous conductivity measurements which can be correlated to diffusivity.[68] If, in aqueous systems, conductivity is increased, it stands to follow that within a hydrogel, those complexes would have the same effect and increase the proton (*i.e.*, hydronium) transport efficiency. Frahn showed that the conductivity of aqueous solutions increased after hydroxy-boric acid complexes were formed; therefore, the increase in hydronium diffusivity observed when comparing Figure 2a,f may be in part due to the increased acidic nature of the PVA−borate complex.[69] Factor 3 was supported by Cassone *et al.*,[34] who state that hydrated calcium ions repelled hydronium ions in aqueous solution and hindered the transport efficiency.

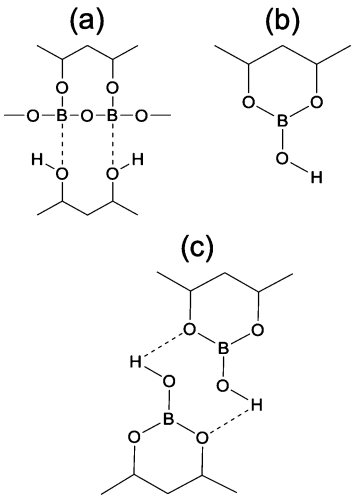

Figure 3. Possible co-existing PVA−borate complexes formed when PVA is crosslinked with saturated boric acid under acidic conditions. (a) 3-coordinate PVA−borate complex. (b) 3-coordinate PVA−borate group. (c) 3-coordinate PVA−borate complex.

Table 1. Water Content and Percentage of Swelling for Each Membrane Type Crosslinked Both Chemically and Physically

membrane	WC (DI) (%)	% swell[a] (DI) (%)	WC (0.1 M) (%)	% swell[a] (0.1 M) (%)	WC (1 M) (%)	% swell[a] (1 M) (%)
10% PVA freeze/thaw	94.1 ± 0.33	−5 ± 8	93.6 ± 0.30	−3 ± 6	87.8 ± 0.06	−18 ± 2
10% PVA/2% Alg freeze/thaw	94.8 ± 0.40	7 ± 4	93.3 ± 0.33	−2 ± 19	88.1 ± 1.11	−5 ± 6
10% PVA chemical	95.8 ± 0.73	30 ± 23	95.1 ± 1.30	28 ± 41	87.5 ± 0.81	−4 ± 10
10% PVA/2% Alg chemical	94.3 ± 0.13	19 ± 4	93.6 ± 0.55	17 ± 9	87.4 ± 0.57	1 ± 3

[a]Negative percent swelling means contraction. Error is based on a 95% confidence interval.

https://doi.org/10.1021/acsestengg.2c00107
ACS EST Engg. XXXX, XXX, XXX−XXX

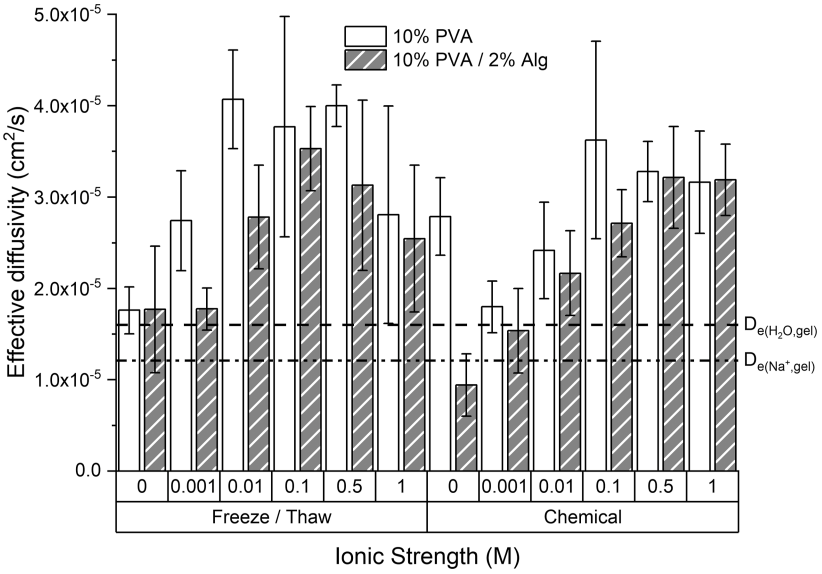

Figure 4. Hydronium effective diffusivity in 10% PVA and 10% PVA/2% Alg hydrogels with different ionic strength solutions and different crosslinking methods. The horizontal lines represent calculated self-diffusion of the given species in a 10% PVA cryogel. Error bars represent a 95% confidence interval. Average diffusivity and error values for each data point can be found in Table S6.

Unlike with 10% PVA, 10% PVA/2% Alg hydrogels did not show a significant change in water content (p = 0.051) after chemical crosslinking, indicating that crosslinking alginate with calcium hindered hydrogel expansion due to the strength and rigidity of the calcium−alginate bond. Cassone *et al.*[34] also found that calcium ions act as "structure makers" in aqueous systems; for example, hydrated calcium ions reinforce water lattice structures, which restricts water rotation, hindering the Grotthuss mechanism. While Cassone *et al.*[34] completed measurements in aqueous systems, the same principles likely apply to hydrogels due to high water content and water domain-dominant transport. No significant differences in hydronium diffusion were observed between 10% PVA and 10% PVA/2% Alg cryogels, so the significant decrease in hydronium diffusivity observed after chemical crosslinking Alg with calcium indicates that interactions between hydronium and calcium are likely the cause. However, longer crosslinking times do change these results as discussed previously. Significant differences in diffusivity were observed in 10% PVA/2% Alg hydrogels with longer crosslinking times (p = 0.0043, Figure 2b−d). Differences can be explained by an interplay between slow kinetics to incorporate boric acid crosslinks (which increase diffusivity) and calcium (which decreases diffusivity). The use of saturated boric acid during crosslinking eliminates crosslinker concentration limitations to complex formation, which has been noted by Miyazaki *et al.*,[70] Nickerson,[71] and Rietjens and Steenbergen,[67] and instead makes time, or diffusion, the limiting factor since boric acid must diffuse through the crosslinked hydrogel to encounter unreacted PVA. Therefore, longer crosslinking times lead to additional PVA−borate complex formation, which in turn causes additional expansion of the water domains within the hydrogel and improves the hydronium transport efficiency.

PVA crosslinked in boric acid has been examined in recent years by Itou *et al.*,[25] Tsai *et al.*,[26] and Wang *et al.*[31] to determine the possible PVA−borate complexes formed under acidic and basic conditions.[25,26,31] The synthesized PVA−borate complex is pH-dependent with the formation of a 3-coordinate complex under acidic conditions and a 4-coordinate complex under basic conditions.[26,31] The crosslinking structures shown in Figure 3 are the most probable complexes formed when PVA is crosslinked with boric acid under acidic conditions.[25,26,31] Itou *et al.*[25] found that Figure 3b,c were the most probable complexes based on Raman analysis of 2,4-pentanediol reacted with boric acid. Tsai *et al.*[26] found that Figure 3a,c were the most probable complexes formed based on Raman and NMR analysis. Wang *et al.*[31] found that Figure 3c was the most likely structure based on Raman and NMR analysis. In summary, Figure 3b,c seem to be the most probable complexes formed by PVA and boric acid crosslinking under the conditions used in this study, although the authors were unable confirm this configuration using FTIR, Raman spectroscopy, or NMR (see the Supporting Information).

Influence of Solvent Ionic Strength on Hydronium Diffusion. The effects of ionic strength on hydronium ion diffusion in 10% PVA and 10% PVA/2% Alg hydrogels are shown in Figure 4. Hydronium diffusion was measured in ionic solutions from 0.001 to 1 M KCl to represent surface water and many natural aquifer systems (0.001−0.01 M) and saline or contaminated aquifers (>0.1 M).[72] Increases in ionic strength produced an increase in effective diffusivity in 10% PVA cryogels up to 0.01 M KCl before leveling off between 0.01 and 0.5 M KCl and decreasing from 0.5 to 1 M KCl. Ionic strength had a significant effect on hydronium diffusivity in 10% PVA cryogels ($p = 4.08 \times 10^{-6}$). Hydronium diffusion through 10% PVA/2% Alg cryogels at low ionic strength was similar to diffusion in DI water. An increase in hydronium ion diffusion in 10% PVA/2% Alg hydrogels was seen when the ionic strength was increased from 0.001 to 0.1 M, began to level off at 0.1−0.5 M, and decreased slightly at 1 M KCl. Ionic strength also had a significant effect on hydronium diffusivity in 10% PVA/2% Alg cryogels ($p = 2.71 \times 10^{-5}$).

Chemically crosslinked 10% PVA hydrogels showed an immediate decrease in hydronium diffusivity at a low ionic strength (0.001 M KCl compared to DI water), bringing the effective diffusivity to similar levels as the equivalent cryogel in DI water. Diffusivity increased from 0.001 to 0.1 M and leveled

https://doi.org/10.1021/acsestengg.2c00107
ACS EST Engg. XXXX, XXX, XXX−XXX

Table 2. Measured and Theoretical Hydronium Diffusivities of Hydronium and Sodium in 10% PVA Hydrogels at 0 M KCl

value type	membrane	solute	crosslinking type	crosslinker	average $\hat{D}$	effective diffusivity (cm^2/s)	± error (cm^2/s)
calculated	10% PVA	H_3O^+	freeze/thaw		0.914	8.50×10^{-5}	1.69×10^{-7}
calculated	10% PVA	H_3O^+	chemical—4.5 h	sat. boric acid	0.939	8.73×10^{-5}	6.42×10^{-7}
calculated	10% PVA	Na^+	freeze/thaw		0.910	1.21×10^{-5}	2.54×10^{-8}
calculated	10% PVA	Na^+	chemical—4.5 h	sat. boric acid	0.888	1.25×10^{-5}	9.65×10^{-8}
measured	10% PVA	H_3O^+	freeze/thaw		0.189	1.76×10^{-5}	2.58×10^{-6}
measured	10% PVA	H_3O^+	chemical—4.5 h	sat. boric acid	0.300	2.79×10^{-5}	4.23×10^{-6}

off between 0.1 and 1 M KCl. Ionic strength had a statistically significant effect on hydronium diffusivity in chemically crosslinked 10% PVA hydrogels ($p = 9.30 \times 10^{-6}$). Alternatively, chemically crosslinked 10% PVA/2% Alg hydrogels showed a steady increase in diffusivity from 0 to 0.5 M before plateauing between 0.5 and 1 M KCl. Ionic strength also had a statistically significant effect on hydronium diffusivity in chemically crosslinked 10% PVA/2% Alg hydrogels ($p = 9.29 \times 10^{-10}$). When sucrose was substituted for KCl at 0.1 M, hydronium effective diffusivity through 10% PVA cryogels was similar to that of hydronium in DI water ($p = 0.896$, Figure S8). This similarity indicated that diffusivity increased as ionic strength increased due to the presence of potassium or chloride ions. NMR, Raman, and FTIR results showed no indication of an interaction between the PVA−borate complex and potassium chloride (Figures S10−S13), indicating that the change in diffusivity observed with increasing ionic strength was driven by potassium/chloride ion−solvent and not potassium/chloride ion−polymer interactions. A diffusion mechanism is proposed and discussed further in the following sections.

A type II, three-way ANOVA (Table S8) was completed for further statistical analysis on the data presented in Figure 4. The ANOVA table showed that each individual factor (membrane type, crosslinking method, and ionic strength) had a significant effect ($p < 0.001$) on hydronium diffusivity. Additionally, when comparing the interactions between each factor, all two-way interactions except the membrane type and crosslinking method ($p = 0.660$) and the three-way interaction were statistically significant. Interaction plots were generated to determine which factor influenced the three-way interaction the most by comparing each factor in a two-way interaction while varying the third factor. All generated interaction plots are available in the Supporting Information (Figures S13−S15). The results of each interaction plot agree that ionic strength has the most significant effect on hydronium diffusivity at low (0−0.001 M KCl) and high (0.1−1 M KCl) ionic strengths and that this effect drove the three-way interaction observed between the membrane type, crosslinking method, and ionic strength. Bioremediation applications would likely introduce these materials into groundwater where the native ionic strength would enhance hydronium diffusivity.

Hydronium Diffusive Theory *Versus* Experimental. A model developed by Lustig and Peppas[33] was used to evaluate the theoretical diffusion coefficient of hydronium through PVA hydrogels. The model has been shown to predict solute diffusion in various hydrogels accurately; however, this model excludes solute−solvent and solute−solute interactions, which are important factors in hydronium mass transfer.[33,38,73]

The measured diffusion in cryogels was 79% less than the theoretical predictions (see Table 2). Likewise, the measured diffusion in boric acid crosslinked 10% PVA hydrogels was 68% less than the theoretical predictions. Since the measured hydronium aqueous diffusivity did not agree with modeled hydronium diffusivity in hydrogels, sodium was used for comparison to predict how a molecule of a similar size and charge would diffuse through a 10% PVA hydrogel without the influence of the Grotthuss mechanism as done previously by Wraight.[49] Using sodium as a surrogate for hydronium diffusion, an effective diffusivity of $1.21 \times 10^{-5} \pm 2.54 \times 10^{-8}$ cm^2/s in 10% PVA cryogels was predicted. The experimental hydronium diffusivity was 45% more than the calculated sodium diffusivity in 10% PVA cryogels ($p = 1.16 \times 10^{-4}$). For cryogels, diffusion coefficients of sodium more closely match that of measured hydronium diffusivity, which suggests that both Brownian motion and Grotthuss mechanisms continue to play a role in diffusion. However, one or both mechanisms are likely hindered within hydrogels since diffusivity in all the hydrogels tested exhibited a slower effective diffusivity than aqueous hydronium diffusion. Roberts[35] found that electrostatic interactions could hinder hydronium transport in aqueous systems, leaving Brownian motion to be the dominant mechanism for diffusion. This result is possible in hydrogel systems too due to the competing interactions from polymer−solvent and solvent−solute interactions and may explain how the Grotthuss mechanism is hindered. In chemically crosslinked 10% PVA, $1.25 \times 10^{-5} \pm 9.65 \times 10^{-8}$ cm^2/s was calculated as the "Brownian only" hydronium diffusivity in hydrogels using sodium as a surrogate. The experimental hydronium diffusivity was 123% greater than that of the calculated sodium diffusivity ($p = 1.59 \times 10^{-5}$). The increase in diffusivity seen when comparing cryogels to boric acid crosslinked hydrogels may be due to an increase in water content. The water content of a hydrogel can increase when the hydrogel is less constrained; in the case of 10% PVA chemically crosslinked hydrogels, the major crosslinker is boric acid which forms non-crystalline PVA−borate complexes. Even though one freeze/thaw cycle is still performed before chemical crosslinking is started, the presence of fewer crystalline domains allows the hydrogel to expand more freely.

A sensitivity analysis of parameters was performed for the model, and the complete analysis is included in the Supporting Information. The influence of solute hydrodynamic radius on hydronium diffusion was examined since hydronium ion complexes can be present in solution in several forms including Zundel and Eigen cations.[74] Additionally, the presence of the charge-balancing chloride ion as a counterion for hydronium may be a potential factor influencing mass transfer.[68] When the hydrodynamic radius of the solute varied from 0.1 to 8 Å at 0 M KCl, the hydronium diffusivity ranged between $8.65-7.56 \times 10^{-5}$ cm^2/s for cryogels and $8.85-8.19 \times 10^{-5}$ cm^2/s for chemically crosslinked hydrogels. At 1 M KCl, the hydronium diffusivity ranged between $8.16-5.54 \times 10^{-5}$ cm^2/s for cryogels and $8.12-5.71 \times 10^{-5}$ cm^2/s for chemically crosslinked hydrogels. A larger hydrodynamic radius was predicted to decrease hydronium diffusion, as expected;

https://doi.org/10.1021/acsestengg.2c00107
ACS EST Engg. XXXX, XXX, XXX−XXX

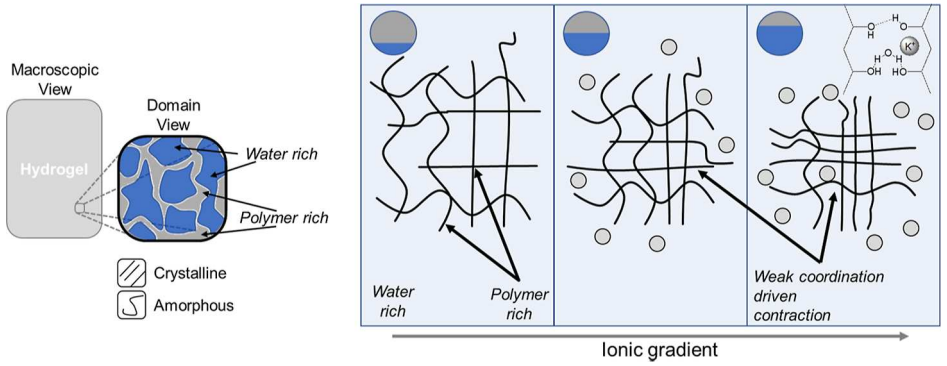

Figure 5. Polymer domain contraction due to coordination between potassium ions (light-gray circles) and PVA hydroxyl groups. Ionic strength is shown to increase from left to right with the upper left-hand circle showing water (blue) and polymer (gray) volume fraction. Crystalline and amorphous regions in the polymer domain are shown and not drawn to scale.

however, the model was not able to predict trends observed with increased ionic strength.

The mesh size was altered indirectly over a wide range of mesh sizes by changing each of the following variables: Flory characteristic ratio (C_n), Flory interaction parameter ($\chi_{\alpha\beta}$), and specific volume of the polymer repeat unit ($\bar{v}$). Sensitivity analysis for mesh size showed that the theoretical model at 0 M KCl from mesh sizes 46 to 565 Å for cryogels and from 71 to 1807 Å for chemically crosslinked hydrogels only altered diffusivity in a range of 8.15−8.62 × 10^{-5} and 8.50−8.83 × 10^{-5} cm^2/s for cryogels and chemically crosslinked hydrogels, respectively. For 1 M KCl, mesh sizes for the same variable ranges were smaller, from 20 to 565 Å in cryogels and from 34 to 1807 Å in chemically crosslinked hydrogels, resulting in a lower predicted range of diffusivities with an increased ionic strength of 7.19−8.00 × 10^{-5} cm^2/s for cryogels and 7.24−7.97 × 10^{-5} cm^2/s. Increased ionic strength was predicted to decrease the mesh size and hydronium diffusion; however, this is counter to what was observed.

Theoretical Hydronium Diffusion Mechanism within the Polymer Domain—Microscale. In polymer systems, hydronium transport may behave different than in strictly aqueous systems due to competing interactions between hydronium, bulk water, and the polymer backbone. Diffusion within, or around, the polymer domain acts as the diffusion-limiting step due to physical obstruction; however, the relatively small size of the hydronium ion (~2.82 Å) in comparison to the mesh size of the hydrogel (~70−340 Å, eq 1) indicates that polymer obstruction via mesh size should not be a significant factor in hydronium diffusion in the hydrogels tested. Solvent−polymer (water−OH hydrogen bonding) and solvent−solute (water−KCl) interactions are postulated to alter the efficiency of diffusion through hydrogel water domains by similar mechanisms to aqueous diffusion as discussed by Huang *et al.*[65] and Patachia *et al.*[64] since diffusion predominately occurs in the water domains of the hydrogel.

In aqueous systems, hydronium ion transport is dependent on the rotation and alignment of water molecules to facilitate Grotthuss transport according to Hassanali *et al.*[73] and Agmon.[38] Bound water, as described by Horne,[75] either in a solvation shell or bound to a hydroxyl group,[63] is inhibited from participating in the Grotthuss mechanism due to its inability to rotate and align with other water molecules. Horne and Axelrod[76] stated that water molecules in the same solvent lattice as the molecules bonded to PVA could be considered bound since their movement was hindered, making the effects of water−hydroxyl hydrogen bonding restricting to hydronium transport. If complexed water molecules are bonded to PVA hydroxyl groups, fewer free water molecules would be available for Grotthuss transport, decreasing the overall efficiency of hydronium diffusion through the hydrogel. When PVA is chemically crosslinked with boric acid, hydrogel expansion due to fewer crystalline regions allows for more water molecules to enter the system and provide additional free water molecules to participate in the Grotthuss mechanism, assuming that PVA hydroxyl groups are already hydrated. Additionally, expanding water domains and the presence of fewer crystalline domains will decrease the probability of polymer obstruction and therefore increase hydronium diffusivity.

According to Patachia *et al.*[64] and Tretinnikov *et al.*,[29] the potassium ion acts as a "structure breaker," the opposite of calcium as a "structure maker." Therefore, when potassium chloride is added to the system, potassium ions will shield PVA hydroxyl groups from water molecules and break water−water hydrogen bonding.[35,64] Roberts[35] states that water can more freely rotate when structure breakers like potassium are present in solution and lattice structures are broken, which in aqueous solutions has been shown to decrease hydronium diffusivity. However, in the case of this study, an increase in diffusivity was observed, which can potentially be explained by potassium ions interacting more favorably with PVA hydroxyl groups over water. When sodium alginate was added to the polymer blend as a cryogel, carboxylate groups on the alginate chain may have chelated free potassium ions in solution, decreasing interactions between potassium ions and hydroxyl groups on PVA. At low concentrations (≤0.1 M), the effects of potassium on the polymer structure were negligible (Table 1), so electrostatic interactions are likely to dominate hydronium diffusion behavior. At high ionic strength, macromolecular changes to the polymer domain became more dominant as the hydrogel physically collapsed. Macromolecular changes to the polymer domain and its effect on hydronium diffusivity will be discussed in the next section.

Theoretical Hydronium Diffusion Mechanism within the Polymer Domain—Macroscale. Figure 5 presents a conceptual model of mass transfer of hydronium within these polymer hydrogels. Hydronium ions transit the hydrogel through regions of water and polymer domains with the latter thought to be the rate-controlling mass-transfer barrier. Lozinsky *et al.*[37] postulate that potassium ions added to increase ionic strength may form weak coordination bonds with hydroxyl groups on PVA, resulting in contraction of the

https://doi.org/10.1021/acsestengg.2c00107
ACS EST Engg. XXXX, XXX, XXX−XXX

polymer domain, decreasing space between water domains, and increasing hydronium effective diffusivity. Tretinnikov *et al.* further postulate that contraction of the polymer domains may lead to the formation of additional crystalline regions once water near these regions was expelled. The contraction process in this case is similar to the formation of crystalline regions during the freeze/thaw process in which ice crystals push PVA chains in close proximity, providing an opportunity for hydrogen bonding. Similar to proteins as described by Lozinsky *et al.*[37] and Hua *et al.*,[36] a polymer "salting out" effect may also explain the observed diffusivity behavior through polymer aggregation and physical contraction, decreasing the volume that hydronium ions must transit between water domains. Hydrogels shrunk by up to 18% after equilibrating in 1 M KCl at room temperature (Table 1). 10% PVA cryogels shrunk by 18%, and 10% PVA/2% Alg chemically crosslinked hydrogels maintained volume or swelled by up to 2%. When 30% PVA cryogels were equilibrated in 0.5 M KCl, hydronium diffusivity decreased when compared to a 10% PVA cryogel under similar conditions (see Figure S20). The observed decrease in diffusivity was likely due to polymer obstruction caused by contraction of the polymer domain, which may have a greater effect on 30% PVA cryogels due to chain mobility of lower-molecular weight PVA, with respect to 10% PVA, and aggregation of crystalline domains (see Figure 5). This result further supported the hypothesis that polymer obstruction was the main factor affecting hydronium diffusivity at high ionic strength. If more crystalline regions are present, the amorphous region will likely push crystalline regions closer together at lower ionic strength in comparison to 10% PVA cryogels as shown by Tretinnikov *et al.*,[29] leading to a decrease in diffusivity as the crystalline regions block direct diffusion pathways. 10% PVA/2% Alg cryogels behaved similar to 10% PVA cryogels in ionic strength solutions greater than 0.001 M KCl once alginate groups were chelated.

Chemically crosslinked PVA exhibits a similar response to increases in ionic strength as PVA cryogels except for low ionic strengths, 0.001 M KCl, when a decrease in diffusivity was observed (Figure 4). The cause of this decrease in diffusivity from 0 to 0.001 M KCl is unknown and requires further investigation. Additional increases in ionic strength from 0.001 to 0.1 M KCl resulted in increases in diffusivity, followed by a plateau from 0.1 to 1 M KCl, where the effects of polymer contraction were limited. Unlike cryogels which were potentially further crosslinked by the formation of additional crystalline domains as the hydrogel contracted, chemically crosslinked PVA was covalently crosslinked by a rigid PVA–borate complex (Figure 3), so when contraction occurred, the formation of crystalline domains was likely hindered by the rigid spacing between PVA chains caused by the presence of PVA–borate complexes as discussed by Miyazaki *et al.*[70] When sodium alginate was crosslinked with calcium chloride, calcium ions bound carboxylate groups together, so the effects of chelation were not observed at any ionic strength. The steady increase in diffusivity from 0 to 0.5 M KCl and the plateau observed from 0.5 to 1 M KCl for 10% PVA/2% Alg chemically crosslinked hydrogels were caused by polymer contraction, similar to 10% PVA chemically crosslinked hydrogels.

In natural encapsulated systems (*e.g.*, biofilms), cell densities can sustain microorganisms up to approximately 10^{11} cells/mL,[77] of which cells occupy 5.5% of the total system volume. The contribution of cells to hindering mass transfer by creating an impermeable fraction of the hydrogel volume is within the error of the current measurements. Alteration of the hydrogel system from actively metabolizing cells, which generate hydronium ions, would be condition-dependent (cell metabolic status, availability of nutrients, cell type, and hydrogel dimension/geometry), as discussed by Westrin and Axelsson.[78] According to Riley *et al.*,[79] quantifying the diffusivity of the solutes of interest in pure hydrogel is necessary to first predict how the solute diffusivity changes based on cell concentration. Hydrogel physical parameters can modify the mesh size, as has been discussed here, which will affect the diffusivity of not only the solute but also the encapsulate microorganisms (*e.g.*, cell leakage from/to hydrogel).

CONCLUSIONS

Co-occurring factors of polymer contraction, solvent–polymer, and solvent–solute interactions were hypothesized to increase hydronium ion diffusivity in hydrogels. When ionic species were added to the solvent, unknown interactions with the PVA–borate complex in 10% PVA hydrogels slowed diffusivity at low ionic strength, but further additions increased diffusivity. Changes in hydronium ion effective diffusivity resulting from the crosslinking type, ionic strength, and polymer formulation can be used to optimize biobead design parameters. Specifically, sizing characteristic length and geometry can minimize acid accumulation within a hydrogel bead when microorganisms are actively generating acid during anaerobic reductive dechlorination. Mass transfer in hydrogels is influenced by polymer composition, solution pH, and concentration and charge of the solute and solvent, allowing for application-specific tunability.[45,59,80−82] The results from this study could also aid in interpretation of and predicting pH gradients within other hydrogel and biological systems including tissue scaffolds,[83] drug release platforms,[84] environmental remediation,[85] encapsulated whole cells, and enzymatic bioprocesses.[86]

ASSOCIATED CONTENT

Supporting Information

The Supporting Information is available free of charge at https://pubs.acs.org/doi/10.1021/acsestengg.2c00107.

Statistical analyses, additional methods, and experimental data (PDF)

AUTHOR INFORMATION

Corresponding Author

James G. Moberly − *Department of Chemical & Biological Engineering, University of Idaho, Moscow, Idaho 83844-1021, United States;* orcid.org/0000-0003-0950-0952; Phone: (208) 885-7705; Email: jgmoberly@uidaho.edu

Authors

Carson J. Silsby − *Department of Chemical & Biological Engineering, University of Idaho, Moscow, Idaho 83844-1021, United States;* orcid.org/0000-0002-1930-6881

Jonathan R. Counts − *Department of Chemical & Biological Engineering, University of Idaho, Moscow, Idaho 83844-1021, United States*

Thomas A. Christensen, II − *Department of Chemical & Biological Engineering, University of Idaho, Moscow, Idaho 83844-1021, United States; College of Veterinary Medicine,*

https://doi.org/10.1021/acsestengg.2c00107
ACS EST Engg. XXXX, XXX, XXX−XXX

Kansas State University, Manhattan, Kansas 66506, United States; orcid.org/0000-0003-1219-9320

Mark F. Roll − *Department of Materials Science & Engineering, University of Idaho, Moscow, Idaho 83844-1011, United States*

Kristopher V. Waynant − *Department of Chemistry, University of Idaho, Moscow, Idaho 83844-2343, United States;* orcid.org/0000-0002-4096-5726

Complete contact information is available at: https://pubs.acs.org/10.1021/acsestengg.2c00107

Author Contributions

CRediT: **Carson J Silsby** formal analysis, investigation, methodology, writing-original draft, writing-review & editing; **Jonathan R. Counts** formal analysis, investigation, methodology; **Thomas A. Christensen II** investigation, methodology, software; **Mark F. Roll** conceptualization, formal analysis, funding acquisition, methodology, project administration, writing-review & editing; **Kristopher V. Waynant** conceptualization, formal analysis, funding acquisition, methodology, project administration, writing-review & editing; **James G Moberly** conceptualization, formal analysis, funding acquisition, methodology, project administration, supervision, visualization, writing-original draft, writing-review & editing.

Notes

The authors declare no competing financial interest.

■ ACKNOWLEDGMENTS

This material is based upon work supported by the National Science Foundation under grant no. 1805358. Any opinions, findings, and conclusions or recommendations expressed in this material are those of the authors and do not necessarily reflect the views of the National Science Foundation. Additional support was provided by an Institutional Development Award (IDeA) from the National Institute of General Medical Sciences of the National Institutes of Health under grant #P20GM103408.

■ REFERENCES

(1) Nikam, S.; Mandal, D. Experimental Study of the Effect of Different Parameters on the Adsorption and Desorption of Trichloroethylene Vapor on Activated Carbon Particles. *ACS Omega* **2020**, *5*, 28080−28087.

(2) Agency for Toxic Substances and Disease Registry (ATSDR). *Toxicological Profile for Trichloroethylene (Update)*; U.S. Public Health Service, U.S. Department of Health and Human Services: Atlanta, GA, 2019.

(3) Mendoza-Sanchez, I.; Autenrieth, R. L.; McDonald, T. J.; Cunningham, J. A. Biological Limitations of Dechlorination of Cis-Dichloroethene during Transport in Porous Media. *Environ. Sci. Technol.* **2018**, *52*, 684−691.

(4) Puentes Jácome, L. A.; Wang, P.-H.; Molenda, O.; Li, Y. X.; Islam, M. A.; Edwards, E. A. Sustained Dechlorination of Vinyl Chloride to Ethene in Dehalococcoides-Enriched Cultures Grown without Addition of Exogenous Vitamins and at Low PH. *Environ. Sci. Technol.* **2019**, *53*, 11364−11374.

(5) Mao, X.; Oremland, R. S.; Liu, T.; Gushgari, S.; Landers, A. A.; Baesman, S. M.; Alvarez-Cohen, L. Acetylene Fuels TCE Reductive Dechlorination by Defined Dehalococcoides/Pelobacter Consortia. *Environ. Sci. Technol.* **2017**, *51*, 2366−2372.

(6) Xiao, Z.; Jiang, W.; Chen, D.; Xu, Y. Bioremediation of Typical Chlorinated Hydrocarbons by Microbial Reductive Dechlorination and Its Key Players: A Review. *Ecotoxicol. Environ. Saf.* **2020**, *202*, 110925.

(7) Ellis, D. E.; Lutz, E. J.; Odom, J. M.; Buchanan, R. J.; Bartlett, C. L.; Lee, M. D.; Harkness, M. R.; DeWeerd, K. A. Bioaugmentation for Accelerated In Situ Anaerobic Bioremediation. *Environ. Sci. Technol.* **2000**, *34*, 2254−2260.

(8) Liu, M.-H.; Hsiao, C.-M.; Lin, C.-E.; Leu, J. Application of Combined In Situ Chemical Reduction and Enhanced Bioremediation to Accelerate TCE Treatment in Groundwater. *Appl. Sci.* **2021**, *11*, 8374.

(9) Liu, P.-W. G.; Wu, Y.-J.; Whang, L.-M.; Lin, T.-F.; Hung, W.-N.; Cho, K.-C. Molecular Tools with Statistical Analysis on Trichloroethylene Remediation Effectiveness. *Int. Biodeterior. Biodegrad.* **2020**, *154*, 105050.

(10) Robinson, C.; Barry, D. A.; McCarty, P. L.; Gerhard, J. I.; Kouznetsova, I. PH Control for Enhanced Reductive Bioremediation of Chlorinated Solvent Source Zones. *Sci. Total Environ.* **2009**, *407*, 4560−4573.

(11) Yu, S.; Semprini, L. Kinetics and Modeling of Reductive Dechlorination at High PCE and TCE Concentrations. *Biotechnol. Bioeng.* **2004**, *88*, 451−464.

(12) Haest, P. J.; Springael, D.; Smolders, E. Dechlorination Kinetics of TCE at Toxic TCE Concentrations: Assessment of Different Models. *Water Res.* **2010**, *44*, 331−339.

(13) Lacroix, E.; Brovelli, A.; Barry, D. A.; Holliger, C. Use of Silicate Minerals for PH Control during Reductive Dechlorination of Chloroethenes in Batch Cultures of Different Microbial Consortia. *Appl. Environ. Microbiol.* **2014**, *80*, 3858−3867.

(14) Charles, C. J.; Rout, S. P.; Patel, K. A.; Akbar, S.; Laws, A. P.; Jackson, B. R.; Boxall, S. A.; Humphreys, P. N. Floc Formation Reduces the PH Stress Experienced by Microorganisms Living in Alkaline Environments. *Appl. Environ. Microbiol.* **2017**, *83*, e02985−16.

(15) Yang, Y.-C.; Huang, W.-S.; Hu, S.-M.; Huang, C.-W.; Chiu, C.-H.; Chen, H.-Y. Synergistic and Regulatable Bioremediation Capsules Fabrication Based on Vapor-Phased Encapsulation of Bacillus Bacteria and Its Regulator by Poly-p-Xylylene. *Polymers* **2020**, *13*, 41.

(16) Valdivia-Rivera, S.; Ayora-Talavera, T.; Lizardi-Jiménez, M. A.; García-Cruz, U.; Cuevas-Bernardino, J. C.; Pacheco, N. Encapsulation of Microorganisms for Bioremediation: Techniques and Carriers. *Rev. Environ. Sci. Biotechnol.* **2021**, *20*, 815−838.

(17) Jen, A. C.; Wake, M. C.; Mikos, A. G. Review: Hydrogels for Cell Immobilization. *Biotechnol. Bioeng.* **1996**, *50*, 357−364.

(18) Zhou, Y.-Z.; Yang, J.; Wang, X.-L.; Pan, Y.-Q.; Li, H.; Zhou, D.; Liu, Y.-D.; Wang, P.; Gu, J.-D.; Lu, Q.; Qiu, Y.-F.; Lin, K.-F. Bio-Beads with Immobilized Anaerobic Bacteria, Zero-Valent Iron, and Active Carbon for the Removal of Trichloroethane from Groundwater. *Environ. Sci. Pollut. Res.* **2014**, *21*, 11500−11509.

(19) Zhou, Y.-Z.; Yang, J.; Wang, X.-L.; Pan, Y.-Q.; Li, H.; Zhou, D.; Liu, Y.-D.; Wang, P.; Gu, J.-D.; Lu, Q.; Qiu, Y.-F.; Lin, K.-F. Bio-Beads with Immobilized Anaerobic Bacteria, Zero-Valent Iron, and Active Carbon for the Removal of Trichloroethane from Groundwater. *Environ. Sci. Pollut. Res.* **2014**, *21*, 11500−11509.

(20) Wang, S.-M.; Tseng, S. Dechlorination of Trichloroethylene by Immobilized Autotrophic Hydrogen-Bacteria and Zero-Valent Iron. *J. Biosci. Bioeng.* **2009**, *107*, 287−292.

(21) Kim, S.; Bae, W.; Hwang, J.; Park, J. Aerobic TCE Degradation by Encapsulated Toluene-Oxidizing Bacteria, Pseudomonas Putida and Bacillus Spp. *Water Sci. Technol.* **2010**, *62*, 1991−1997.

(22) Schuszter, G.; Gehér-Herczegh, T.; Szűcs, Á.; Tóth, Á.; Horváth, D. Determination of the Diffusion Coefficient of Hydrogen Ion in Hydrogels. *Phys. Chem. Chem. Phys.* **2017**, *19*, 12136−12143.

(23) Choudhury, R. R.; Gohil, J. M.; Dutta, K. Poly(Vinyl Alcohol)-Based Membranes for Fuel Cell and Water Treatment Applications: A Review on Recent Advancements. *Polym. Adv. Technol.* **2021**, *32*, 4175−4203.

(24) Ajith, C.; Deshpande, A. P.; Varughese, S. Proton Conductivity in Crosslinked Hydrophilic Ionic Polymer System: Competitive Hydration, Crosslink Heterogeneity, and Ineffective Domains. *J. Polym. Sci., Part B: Polym. Phys.* **2016**, *54*, 1087−1101.

(25) Itou, T.; Kitai, H.; Shimazu, A.; Miyazaki, T.; Tashiro, K. Clarification of Cross-Linkage Structure in Boric Acid Doped Poly(Vinyl Alcohol) and Its Model Compound As Studied by an Organized Combination of X-Ray Single-Crystal Structure Analysis, Raman Spectroscopy, and Density Functional Theoretical Calculation. *J. Phys. Chem. B* **2014**, *118*, 6032−6037.
(26) Tsai, C.-J.; Chang, Y.-R.; Lee, D.-J. Shape Stable Poly(Vinyl Alcohol) and Alginate Cross-Linked Hydrogel under Drying-Rewetting Cycles: Boron Substitution. *Ind. Eng. Chem. Res.* **2018**, *57*, 14213−14222.
(27) Chang, C.-C.; Tseng, S.-K. Immobilization of Alcaligenes Eutrophus Using PVA Crosslinked with Sodium Nitrate. *Biotechnol. Tech.* **1998**, *12*, 865−868.
(28) Chang, C.; Lue, A.; Zhang, L. Effects of Crosslinking Methods on Structure and Properties of Cellulose/PVA Hydrogels. *Macromol. Chem. Phys.* **2008**, *209*, 1266−1273.
(29) Tretinnikov, O. N.; Sushko, N. I.; Zagorskaya, S. A. Effect of Salt Concentration on the Structure of Poly(Vinyl Alcohol) Cryogels Obtained from Aqueous Salt Solutions. *J. Appl. Spectrosc.* **2015**, *82*, 40−45.
(30) Harland, R. S.; Peppas, N. A. Solute Diffusion in Swollen Membranes VII. Diffusion in Semicrystalline Networks. *Colloid Polym. Sci.* **1989**, *267*, 218−225.
(31) Wang, P.-H.; Chang, Y.-R.; Lee, D.-J. Structure for Shape Stable Poly(Vinyl Alcohol) Hydrogel under PH Shock. *J. Taiwan Inst. Chem. Eng.* **2019**, *104*, 341−350.
(32) Wang, X.; You, J.; Wu, Y. In Situ Gelation of Aqueous Sulfuric Acid Solution for Fuel Cells. *RSC Adv.* **2021**, *11*, 22461−22466.
(33) Lustig, S. R.; Peppas, N. A. Solute Diffusion in Swollen Membranes. IX. Scaling Laws for Solute Diffusion in Gels. *J. Appl. Polym. Sci.* **1988**, *36*, 735−747.
(34) Cassone, G.; Creazzo, F.; Saija, F. Ionic Diffusion and Proton Transfer of MgCl2 and CaCl2 Aqueous Solutions: An Ab Initio Study under Electric Field. *Mol. Simul.* **2019**, *45*, 373−380.
(35) Roberts, N. K. Proton Diffusion and Activity in the Presence of Electrolytes. *J. Phys. Chem.* **1976**, *80*, 1117−1120.
(36) Hua, M.; Wu, S.; Ma, Y.; Zhao, Y.; Chen, Z.; Frenkel, I.; Strzalka, J.; Zhou, H.; Zhu, X.; He, X. Strong Tough Hydrogels via the Synergy of Freeze-Casting and Salting Out. *Nature* **2021**, *590*, 594−599.
(37) Lozinsky, V. I.; Sakhno, N. G.; Damshkaln, L. G.; Bakeeva, I. V.; Zubov, V. P.; Kurochkin, I. N.; Kurochkin, I. I. Study of Cryostructuring of Polymer Systems: 31. Effect of Additives of Alkali Metal Chlorides on Physicochemical Properties and Morphology of Poly(Vinyl Alcohol) Cryogels. *Colloid J.* **2011**, *73*, 234.
(38) Agmon, N. The Grotthuss Mechanism. *Chem. Phys. Lett.* **1995**, *244*, 456−462.
(39) Roberts, N. K.; Zundel, G. IR studies of long-range surface effects—excess proton mobility in water in quartz pores|Nature. https://www.nature.com/articles/278726a0 (accessed March 31, 2022).
(40) Holloway, J. L.; Lowman, A. M.; Palmese, G. R. The Role of Crystallization and Phase Separation in the Formation of Physically Cross-Linked PVA Hydrogels. *Soft Matter* **2013**, *9*, 826−833.
(41) Wu, K.-Y. A.; Wisecarver, K. D. Cell Immobilization Using PVA Crosslinked with Boric Acid. *Biotechnol. Bioeng.* **1992**, *39*, 447−449.
(42) Northrop, J. H.; Anson, M. L. A Method for the Determination of Diffusion Constants and the Calculation of the Radius and Weight of the Hemoglobin Molecule. *J. Gen. Physiol.* **1929**, *12*, 543−554.
(43) Meadows, D. L.; Peppas, N. A. Solute Diffusion in Swollen Membranes Iii. Non-Equilibrium Thermodynamic Aspects of Solute Diffusion in Polymer Network Membranes. *Chem. Eng. Commun.* **1984**, *31*, 101−119.
(44) Peppas, N. A.; Merrill, E. W. Poly(Vinyl Alcohol) Hydrogels: Reinforcement of Radiation-Crosslinked Networks by Crystallization. *J. Polym. Sci., Polym. Chem. Ed.* **1976**, *14*, 441−457.
(45) Gudeman, L. F.; Peppas, N. A. Preparation and Characterization of PH-Sensitive, Interpenetrating Networks of Poly(Vinyl Alcohol) and Poly(Acrylic Acid). *J. Appl. Polym. Sci.* **1995**, *55*, 919−928.
(46) Nightingale, E. R. Phenomenological Theory of Ion Solvation. Effective Radii of Hydrated Ions. *J. Phys. Chem.* **1959**, *63*, 1381−1387.
(47) Masaro, L.; Ousalem, M.; Baille, W. E.; Lessard, D.; Zhu, X. X. Self-Diffusion Studies of Water and Poly(Ethylene Glycol) in Solutions and Gels of Selected Hydrophilic Polymers. *Macromolecules* **1999**, *32*, 4375−4382.
(48) Zhang; Han. Viscosity and Density of Water + Sodium Chloride + Potassium Chloride Solutions at 298.15 K. *J. Chem. Eng. Data* **1996**, *41*, 516−520.
(49) Wraight, C. A. Chance and Design—Proton Transfer in Water, Channels and Bioenergetic Proteins. *Biochim. Biophys. Acta, Bioenerg.* **2006**, *1757*, 886−912.
(50) Masaro, L.; Zhu, X. X. Physical Models of Diffusion for Polymer Solutions, Gels and Solids. *Prog. Polym. Sci.* **1999**, *24*, 731−775.
(51) Sinton, S. W. Complexation Chemistry of Sodium Borate with Poly(Vinyl Alcohol) and Small Diols: A Boron-11 NMR Study. *Macromolecules* **1987**, *20*, 2430−2441.
(52) R Core Team. *R: A Language and Environment for Statistical Computing*; R Foundation for Statistical Computing: Vienna, Austria, 2021. https://www.R-project.org/.
(53) Fox, J.; Weisberg, S. *An R Companion to Applied Regression*, 3rd ed.; Sage: Thousand Oaks CA, 2019. https://socialsciences.mcmaster.ca/jfox/Books/Companion/.
(54) Hothorn, T.; Bretz, F.; Westfall, P. Simultaneous Inference in General Parametric Models. *Biom. J.* **2008**, *50*, 346−363.
(55) De Rosario-Martinez, H. phia: Post-Hoc Interaction Analysis. R package version 0.2-1. 2015, https://CRAN.R-project.org/package=phia.
(56) Singmann, H.; Bolker, B.; Westfall, J.; Aust, F.; Ben-Shachar, M. S. afex: Analysis of Factorial Experiments. R package version 1.0-1. 2021, https://CRAN.R-project.org/package=afex.
(57) Lenth, R. V. Emmeans: Estimated Marginal Means, Aka Least-Squares Means. R package version 1.7.0. 2021, https://CRAN.R-project.org/package=emmeans.
(58) Hoare, T. R.; Kohane, D. S. Hydrogels in Drug Delivery: Progress and Challenges. *Polymer* **2008**, *49*, 1993−2007.
(59) Fatin-Rouge, N.; Milon, A.; Buffle, J.; Goulet, R. R.; Tessier, A. Diffusion and Partitioning of Solutes in Agarose Hydrogels: The Relative Influence of Electrostatic and Specific Interactions. *J. Phys. Chem. B* **2003**, *107*, 12126−12137.
(60) Kapellos, G. E.; Alexiou, T. S.; Payatakes, A. C. A Multiscale Theoretical Model for Diffusive Mass Transfer in Cellular Biological Media. *Math. Biosci.* **2007**, *210*, 177−237.
(61) Harland, R. S.; Peppas, N. A. Solute Diffusion in Swollen Membranes. *Polym. Bull.* **1987**, *18*, 553−556.
(62) Peterlin, A. Dependence of Diffusive Transport on Morphology of Crystalline Polymers. *J. Macromol. Sci., Part B: Phys.* **1975**, *11*, 57−87.
(63) Ricciardi, R.; Auriemma, F.; De Rosa, C.; Lauprêtre, F. X-Ray Diffraction Analysis of Poly(Vinyl Alcohol) Hydrogels, Obtained by Freezing and Thawing Techniques. *Macromolecules* **2004**, *37*, 1921−1927.
(64) Patachia, S.; Valente, A. J. M.; Baciu, C. Effect of Non-Associated Electrolyte Solutions on the Behaviour of Poly(Vinyl Alcohol)-Based Hydrogels. *Eur. Polym. J.* **2007**, *43*, 460−467.
(65) Huang, Y.; Zhang, M.; Ruan, W. High-Water-Content Graphene Oxide/Polyvinyl Alcohol Hydrogel with Excellent Mechanical Properties. *J. Mater. Chem. A* **2014**, *2*, 10508−10515.
(66) Gayet, J.-C.; Fortier, G. High Water Content BSA-PEG Hydrogel for Controlled Release Device: Evaluation of the Drug Release Properties. *J. Controlled Release* **1996**, *38*, 177−184.
(67) Rietjens, M.; Steenbergen, P. A. Crosslinking Mechanism of Boric Acid with Diols Revisited. *Eur. J. Inorg. Chem.* **2005**, *2005*, 1162−1174.

https://doi.org/10.1021/acsestengg.2c00107
ACS EST Engg. XXXX, XXX, XXX−XXX

(68) Kamcev, J.; Paul, D. R.; Manning, G. S.; Freeman, B. D. Ion Diffusion Coefficients in Ion Exchange Membranes: Significance of Counterion Condensation. *Macromolecules* **2018**, *51*, 5519−5529.
(69) Frahn, J. L. Paper Electrophoresis of Hydroxycarboxylic Acids as Their Borate Complexes with Special Reference to Viridifloric, Trachelanthic, Lasiocarpic and Heliotric Acids: The Importance of the "Gem- Dialkyl" Effect in Complex Formation. *J. Chromatogr. A* **1984**, *314*, 167−181.
(70) Miyazaki, T.; Takeda, Y.; Akane, S.; Itou, T.; Hoshiko, A.; En, K. Role of Boric Acid for a Poly (Vinyl Alcohol) Film as a Cross-Linking Agent: Melting Behaviors of the Films with Boric Acid. *Polymer* **2010**, *51*, 5539−5549.
(71) Nickerson, R. F. Thickening of Poly(Vinyl Alcohol) by Borate. *J. Appl. Polym. Sci.* **1971**, *15*, 111−116.
(72) Polemio, M.; Bufo, S.; Paoletti, S. Evaluation of Ionic Strength and Salinity of Groundwaters: Effect of the Ionic Composition. *Geochim. Cosmochim. Acta* **1980**, *44*, 809−814.
(73) Hassanali, A.; Giberti, F.; Cuny, J.; Kühne, T. D.; Parrinello, M. Proton Transfer through the Water Gossamer. *Proc. Natl. Acad. Sci. U.S.A.* **2013**, *110*, 13723−13728.
(74) Kornyshev, A. A.; Kuznetsov, A. M.; Spohr, E.; Ulstrup, J. Kinetics of Proton Transport in Water. *J. Phys. Chem. B* **2003**, *107*, 3351−3366.
(75) Horne, R. A. Electrical Conductance in Acidic, Aqueous Solutions. *J. Electrochem. Soc.* **1965**, *112*, 857.
(76) Horne, R. A.; Axelrod, E. H. Proton Mobility and Electron Exchange in Aqueous Media. *J. Chem. Phys.* **1964**, *40*, 1518−1522.
(77) Hou, J.; Wang, C.; Rozenbaum, R. T.; Gusnaniar, N.; de Jong, E. D.; Woudstra, W.; Geertsema-Doornbusch, G. I.; Atema-Smit, J.; Sjollema, J.; Ren, Y.; Busscher, H. J.; van der Mei, H. C. Bacterial Density and Biofilm Structure Determined by Optical Coherence Tomography. *Sci. Rep.* **2019**, *9*, 9794.
(78) Westrin, B. A.; Axelsson, A. Diffusion in Gels Containing Immobilized Cells: A Critical Review. *Biotechnol. Bioeng.* **1991**, *38*, 439−446.
(79) Riley, M. R.; Muzzio, F. J.; Buettner, H. M.; Reyes, S. C. A Simple Correlation for Predicting Effective Diffusivities in Immobilized Cell Systems. *Biotechnol. Bioeng.* **1996**, *49*, 223−227.
(80) Hagel, V.; Haraszti, T.; Boehm, H. Diffusion and Interaction in PEG-DA Hydrogels. *Biointerphases* **2013**, *8*, 36.
(81) Risbud, M. V.; Hardikar, A. A.; Bhat, S. V.; Bhonde, R. R. PH-Sensitive Freeze-Dried Chitosan−Polyvinyl Pyrrolidone Hydrogels as Controlled Release System for Antibiotic Delivery. *J. Controlled Release* **2000**, *68*, 23−30.
(82) Cha, R.; He, Z.; Ni, Y. Preparation and Characterization of Thermal/PH-Sensitive Hydrogel from Carboxylated Nanocrystalline Cellulose. *Carbohydr. Polym.* **2012**, *88*, 713−718.
(83) Bharadwaz, A.; Jayasuriya, A. C. Recent Trends in the Application of Widely Used Natural and Synthetic Polymer Nanocomposites in Bone Tissue Regeneration. *Mater. Sci. Eng., C* **2020**, *110*, 110698.
(84) Zhu, Y.-J.; Chen, F. PH-Responsive Drug-Delivery Systems. *Chem.—Asian J.* **2015**, *10*, 284−305.
(85) Robinson, C.; Barry, D. A. Design Tool for Estimation of Buffer Requirement for Enhanced Reductive Dechlorination of Chlorinated Solvents in Groundwater. *Environ. Model. Softw.* **2009**, *24*, 1332−1338.
(86) Pierre, A. C. The Sol-Gel Encapsulation of Enzymes. *Biocatal. Biotransform.* **2004**, *22*, 145−170.

https://doi.org/10.1021/acsestengg.2c00107
ACS EST Engg. XXXX, XXX, XXX−XXX